Supplementary Information

Cobalt complex with tetradentate aminopyridine ligand: A single-component and efficient catalytic system for cycloaddition reactions of CO_2 and epoxides

Ning Yu,[a] Bowen Zhang,[a,b] Shuyan Liang,[a] Minghui Shi,[a] Feng Han,[a,*] Congcong Zhang,[a,*] Qingfeng Yang[c] and Chengxia Miao[a,*]

[a] Key Laboratory of Low-Carbon and Green Agriculture Chemistry in Universities of Shandong, College of Chemistry and Material Science, Shandong Agricultural University, Tai'an, Shandong 271018, P. R. China

[b] Department of Chemistry, Texas A&M University, College Station, Texas 77843, United States

[c] State Key Laboratory of High-Efficiency Utilization of Coal and Green Chemical Engineering, Ningxia University, Yinchuan, 750021, Ningxia, China

* Corresponding authors: fenghan@sdau.edu.cn, cczhang@sdau.edu.cn, chxmiao@sdau.edu.cn

E-mail: fenghan@sdau.edu.cn (F. Han), cczhang@sdau.edu.cn (C. Zhang), chxmiao@sdau.edu.cn (C. Miao)

Table of Contents

1. Part Data for Screening the Reaction Conditions

Table S1. Screening the Ratios of 3b:$CoBr_2$ for the Cycloaddition Reaction between Styrene Oxide and CO_2[a]

Entry	**3b** (mol%)	$CoBr_2$ (mol%)	Conversion (%)[b]	Yield (%)[b]	Selectivity (%)[b]
1	1	1	73	72	99
2	3	3	78	75	96
3	5	5	94	93	99
4	7	7	95	85	89
5	5	10	96	74	77
6	5	2.5	84	80	95

[a] Reaction conditions: 1 mmol styrene oxide and 2.5 MPa CO_2 were catalyzed by certain amount of **3b** and $CoBr_2$ in CH_3CN at 90 °C for 8 h. [b] Determined by gas chromatography using biphenyl as the internal standard.

Table S2. Exploring the Solvent Effect on the Cycloaddition Reaction Between Styrene Oxide and CO_2[a]

Entry	Solvent	Conversion (%)[b]	Yield (%)[b]	Selectivity (%)[b]
1	CH_3CN	94	93	99
2	DCE	88	78	89
3	Toluene	81	70	86
4	MeOH	90	62	69
5	DMC	83	81	98
6	DMF	98	79	81
7	THF	88	79	90

[a] Reaction conditions: 1 mmol styrene oxide and 2.5 MPa CO_2 were catalyzed by 5 mol% of **3b** and 5 mol% of $CoBr_2$ in certain solvent at 90 °C for 8 h. [b] Determined by gas chromatography using biphenyl as the internal standard.

Table S3. Exploring the Reaction Time on the Cycloaddition Reaction Between Styrene Oxide and CO_2[a]

Entry	T (h)	Conversion (%)[b]	Yield (%)[b]	Selectivity (%)[b]
1	6	92	88	96
2	7	93	89	96
3	8	94	93	99
4	9	92	90	98
5	10	93	91	98

[a] Reaction conditions: 1 mmol styrene oxide and 2.5 MPa CO_2 were catalyzed by 5 mol% of **3b** and 5 mol% of $CoBr_2$ in CH_3CN at 90 °C for several hours. [b] Determined by gas chromatography using biphenyl as the internal standard.

Table S4. Exploring the Reactivity of Catalyst at a Short Time on the Cycloaddition Reaction Between Styrene Oxide and CO_2[a]

Entry	catalyst	Conversion (%)[b]	Yield (%)[b]	Selectivity (%)[b]
1	**3a-Co**	88	68	77
2	**3b-Co**	95	90	95
3	**3c-Co**	96	91	95

[a] Reaction conditions: 1 mmol styrene oxide and 2.5 MPa CO_2 were catalyzed by 5 mol% of catalyst at 90 °C for 2 hours in absence of solvent. [b] Determined by gas chromatography using biphenyl as the internal standard.

2. The crystalline data of 3a-Co

Table S5. Data Collection and Structure Refinement for 3a-Co

Name	Data
Empirical formula	C_{20} H_{28} Br_2 Co N_4
Formula weight	543.21
Space group	P 43 21 2
a, Å	9.19310(10)
b, Å	9.19310(10)
c, Å	23.9143(4)
α, deg	90
β, deg	90
γ, deg	90
V, Å^3	2021.07(6)
Z	4
temp, K	100.01(10)
λ (Cu *Kα*), Å	1.54184
D, g cm^{-3}	1.785
Final R indices [I>2sigma(I)]	R1 = 0.0286, wR2 = 0.0717
R indices (all data)	R1 = 0.0300, wR2 = 0.0723

Table S6. Selected Bond Distances (Å) and Angles (º) for 3a-Co

Bond Distances (Å)	
Co1-N1	2.157(3)
Co1-N2	2.157(3)
Co1-N3	2.218(4)
Co1-N4	2.218(4)
Co1 Br1	2.5850(7)
Bond Angles (º)	
Br1-Co1-Br1	94.24(4)
N1-Co1-Br1	89.55(9)
N1-Co1-Br1	89.55(9)
N1-Co1-Br1	97.16(9)
N1-Co1-Br1	97.16(9)
N1-Co1-N1	170.16(18)
N1-Co1-N2	76.69(12)
N1-Co1-N2	95.68(12)
N1-Co1-N2	95.68(12)
N1-Co1-N2	76.69(12)
N2-Co1-Br1	170.33(8)
N2-Co1-Br1	170.33(8)
N2-Co1-Br1	93.18(9)
N2-Co1-Br1	93.18(9)
N2-Co1-N2	80.16(18)

3. The crystalline data of 3b-Co

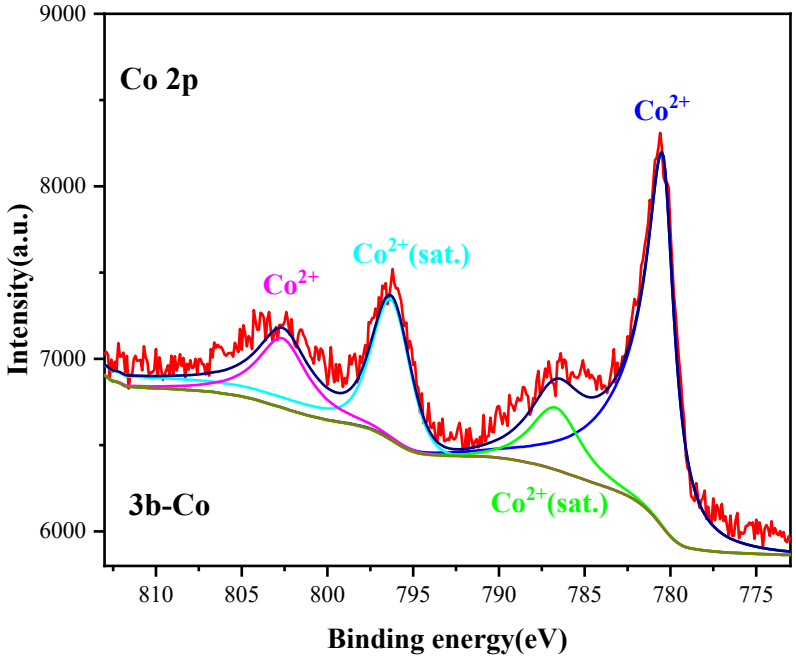

Figure S1. XPS of **3b-Co.**

4. The Gas Spectra of Cycloaddition Reaction Between 4a and CO_2

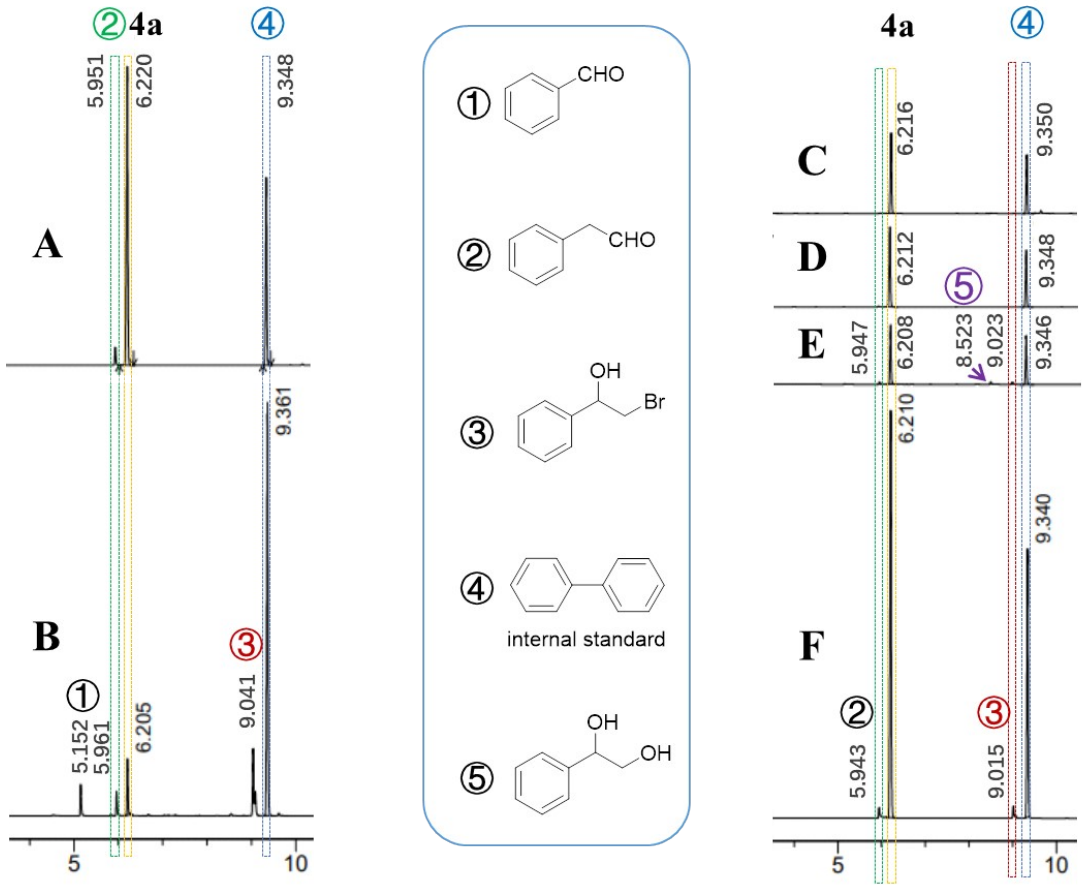

Figure S2. The gas chromatogram of cycloaddition reaction between **4a** and CO_2 under various conditions: ligand **3b** (5 mol%) (A, table 1, entry 4) or $CoBr_2$ (5 mol%) (B, table 1, entry 5) was used separately; CoF_2 (C, table 1, entry 15); $Co(OAc)_2$ (D, table 1, entry 16); 0.1 MPa CO_2 (E, table 1, entry 17); 25 ^oC (F, table 1, entry 6).

5. Copies of ^{1}H and ^{13}C NMR Spectra

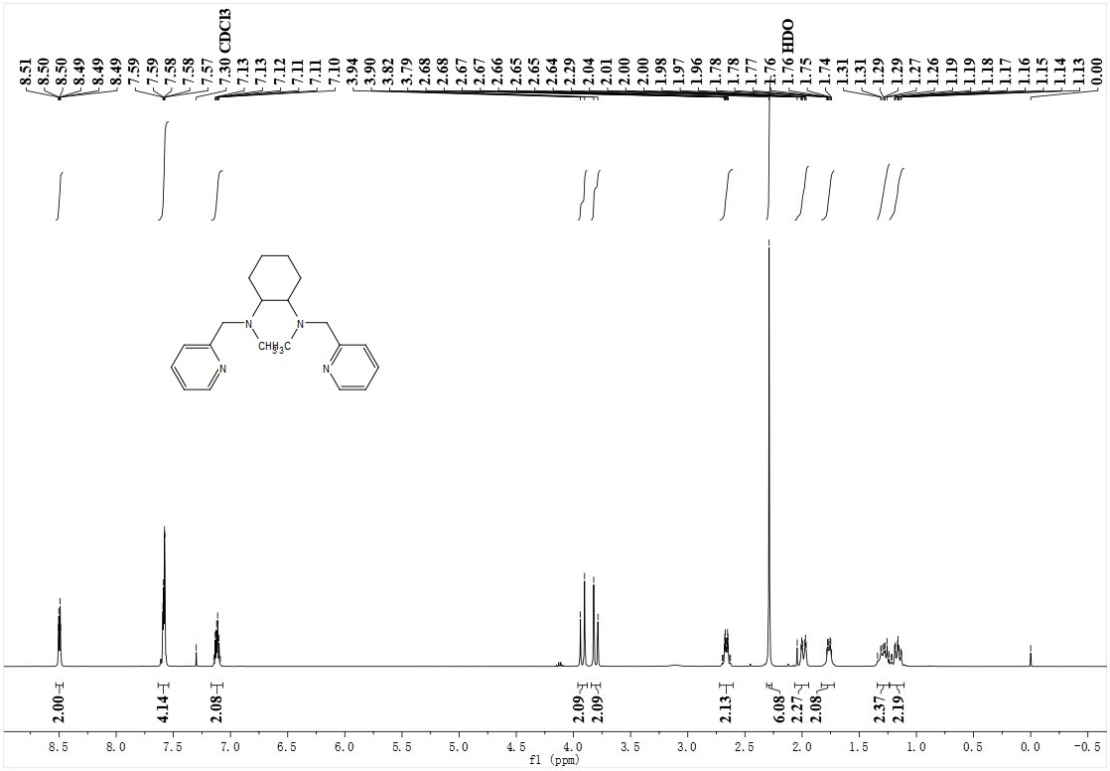

Figure S3. ^{1}H NMR spectrum of **3a**

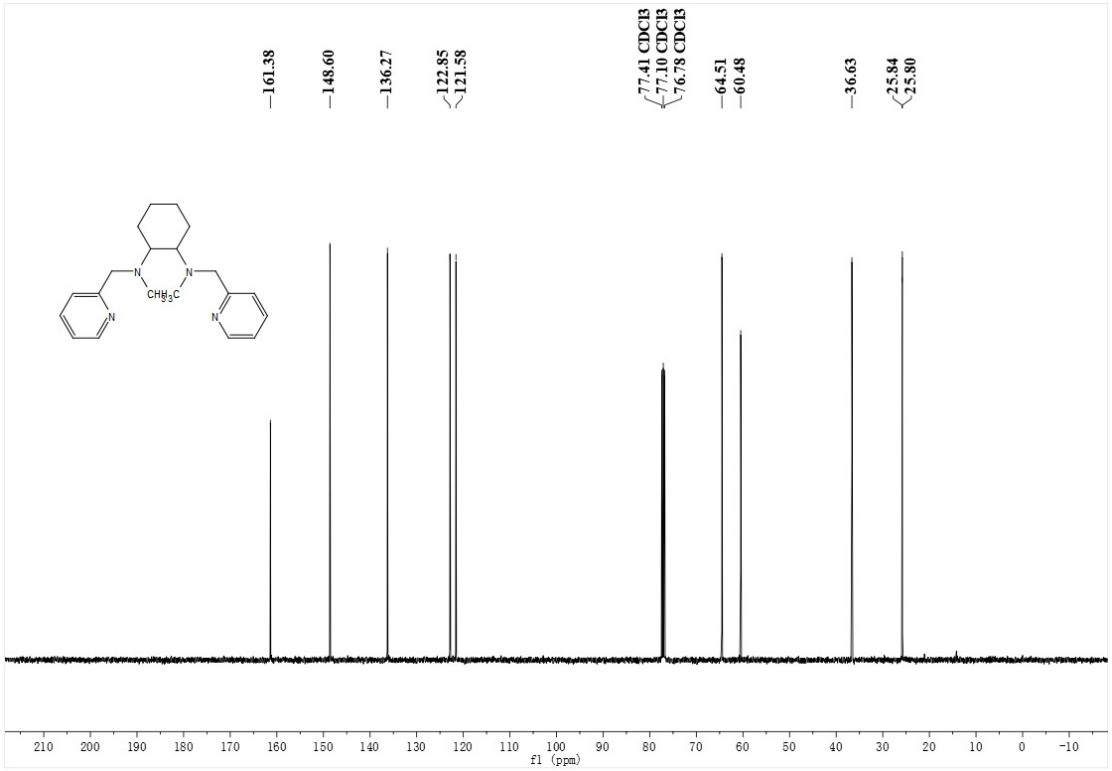

Figure S4. ^{13}C NMR spectrum of **3a**

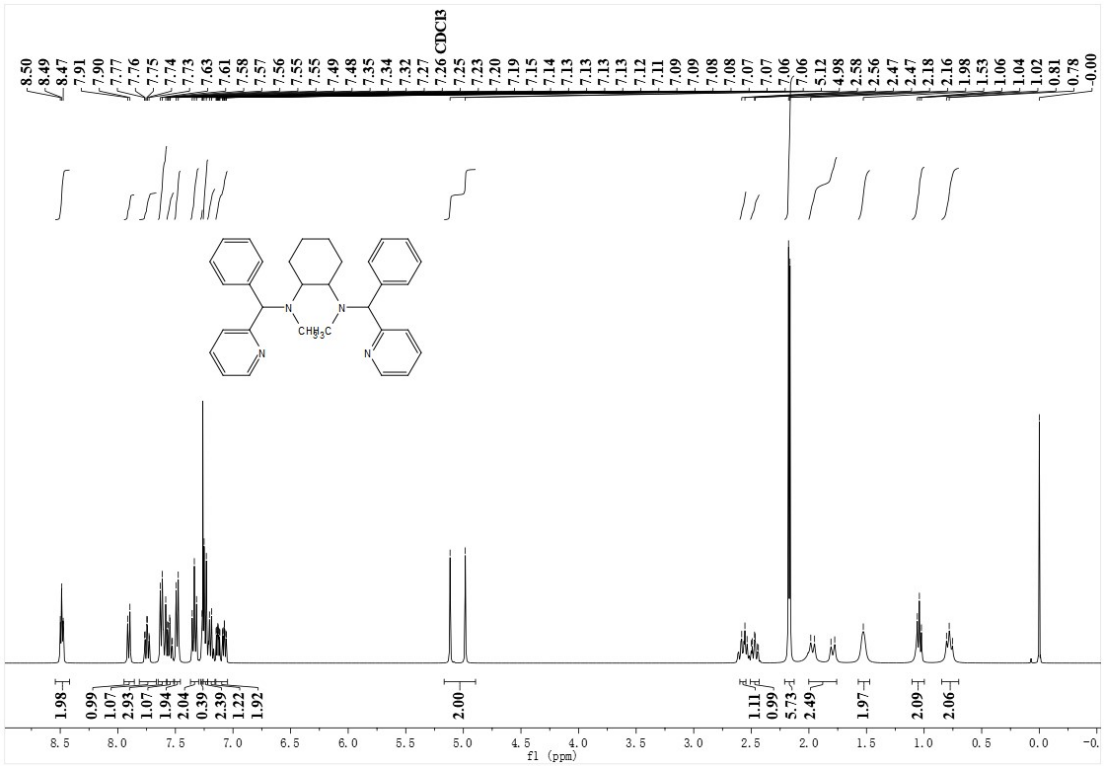

Figure S5. ^{1}H NMR spectrum of **3b**

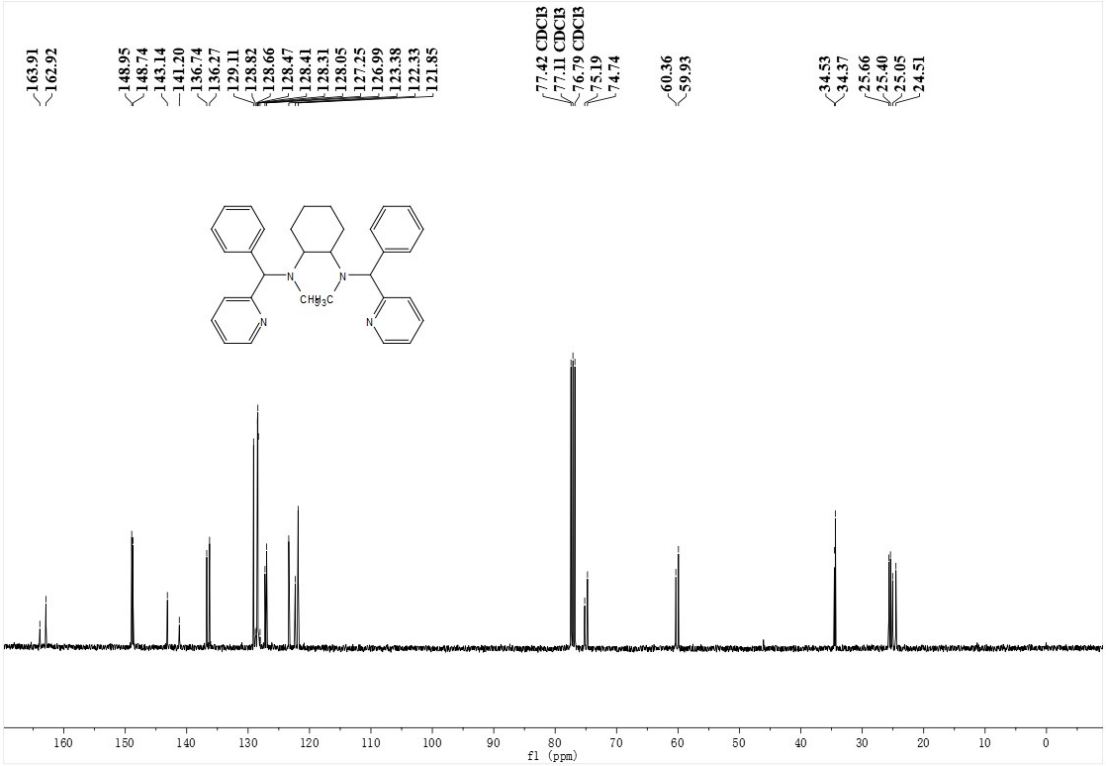

Figure S6. ^{13}C NMR spectrum of **3b**

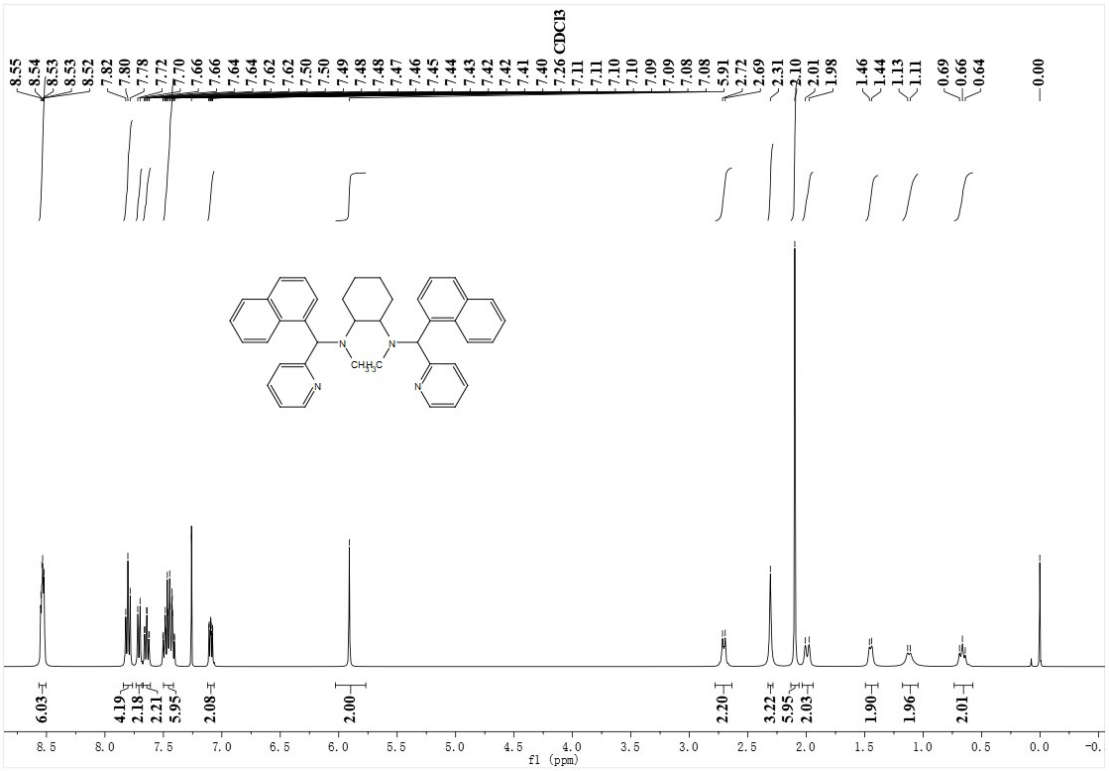

Figure S7. ^{1}H NMR spectrum of **3c**

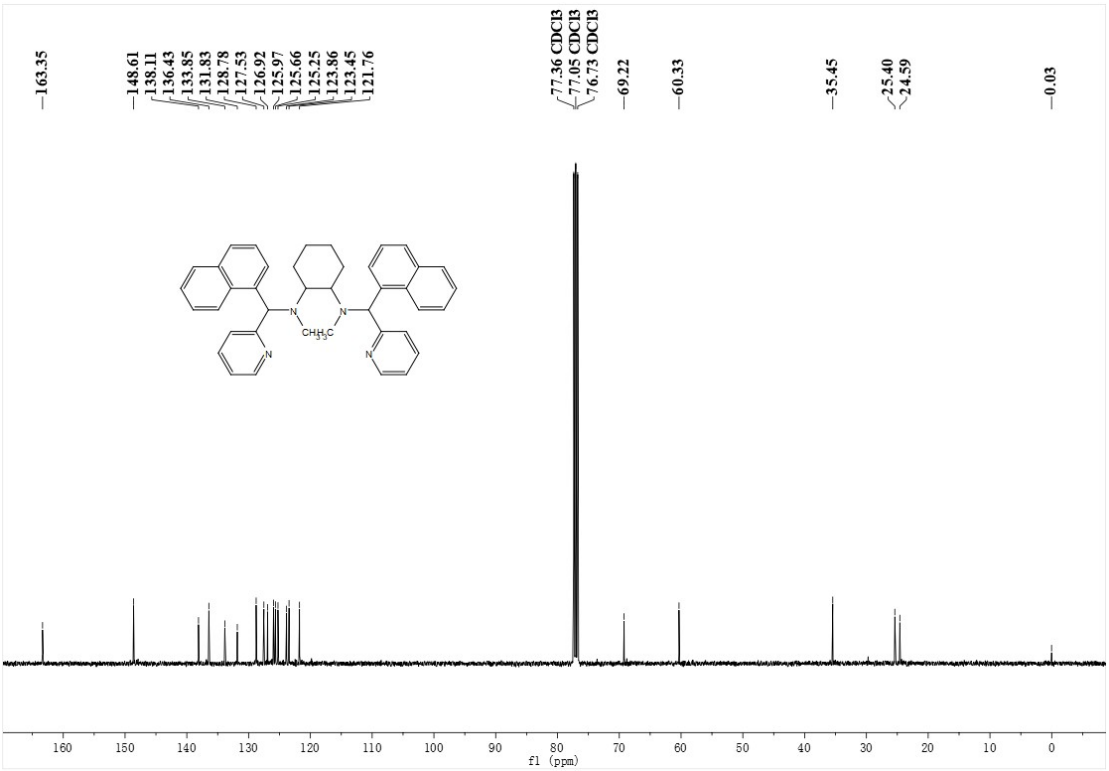

Figure S8. ^{13}C NMR spectrum of **3c**

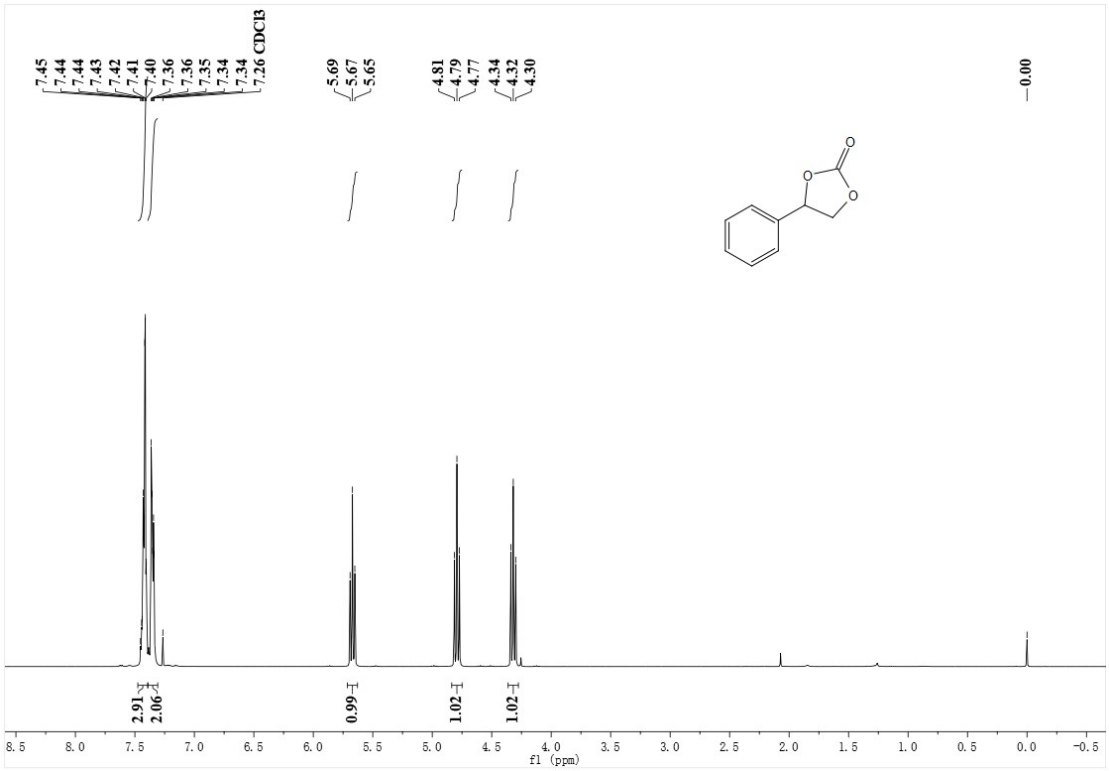

Figure S9. ^{1}H NMR spectrum of **5a**

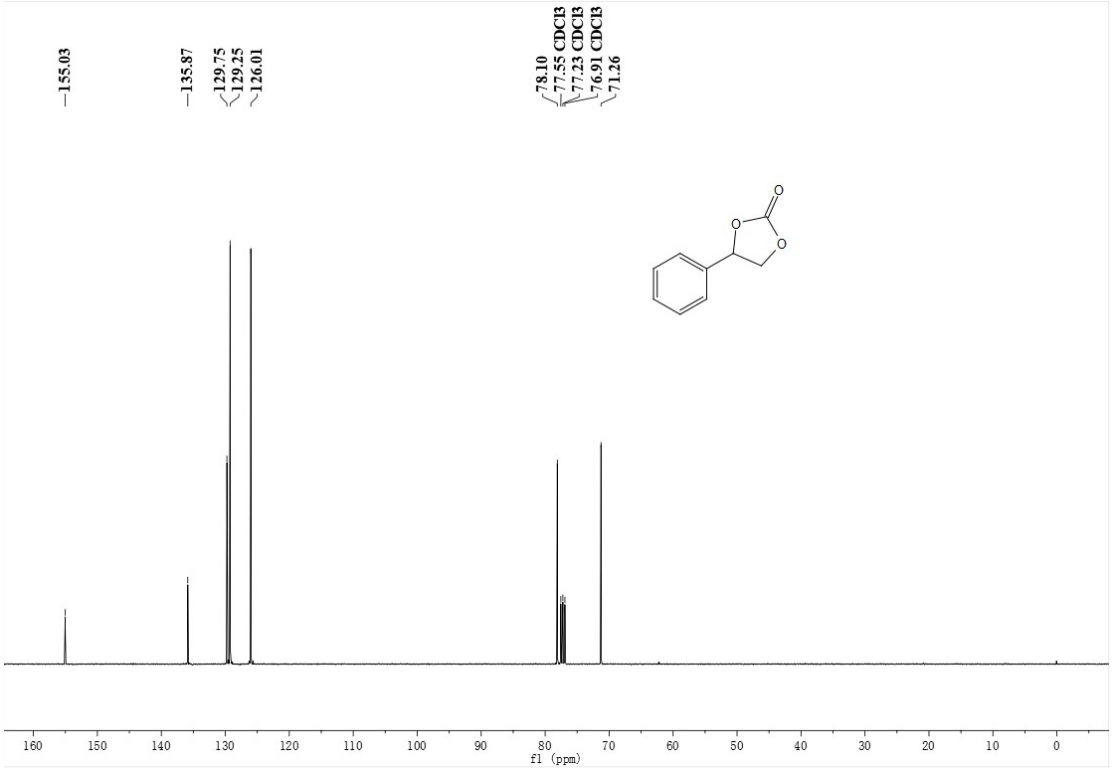

Figure S10. ^{13}C NMR spectrum of **5a**

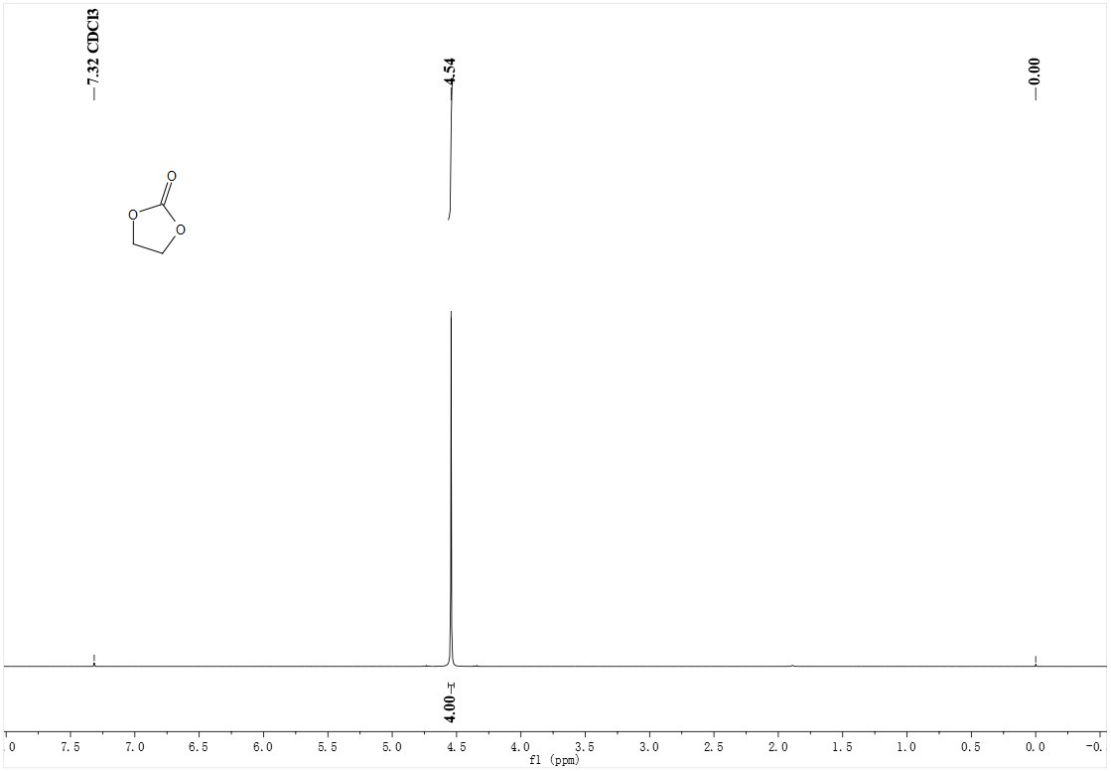

Figure S11. ^{1}H NMR spectrum of **5b**

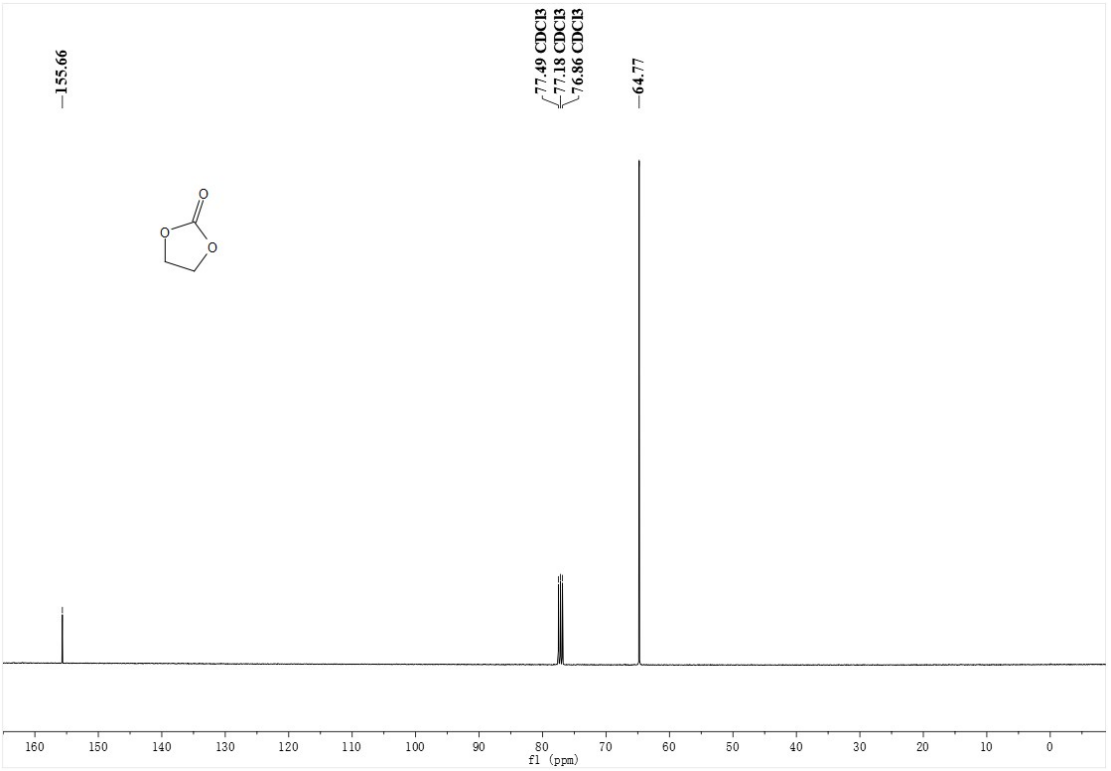

Figure S12. ^{13}C NMR spectrum of **5b**

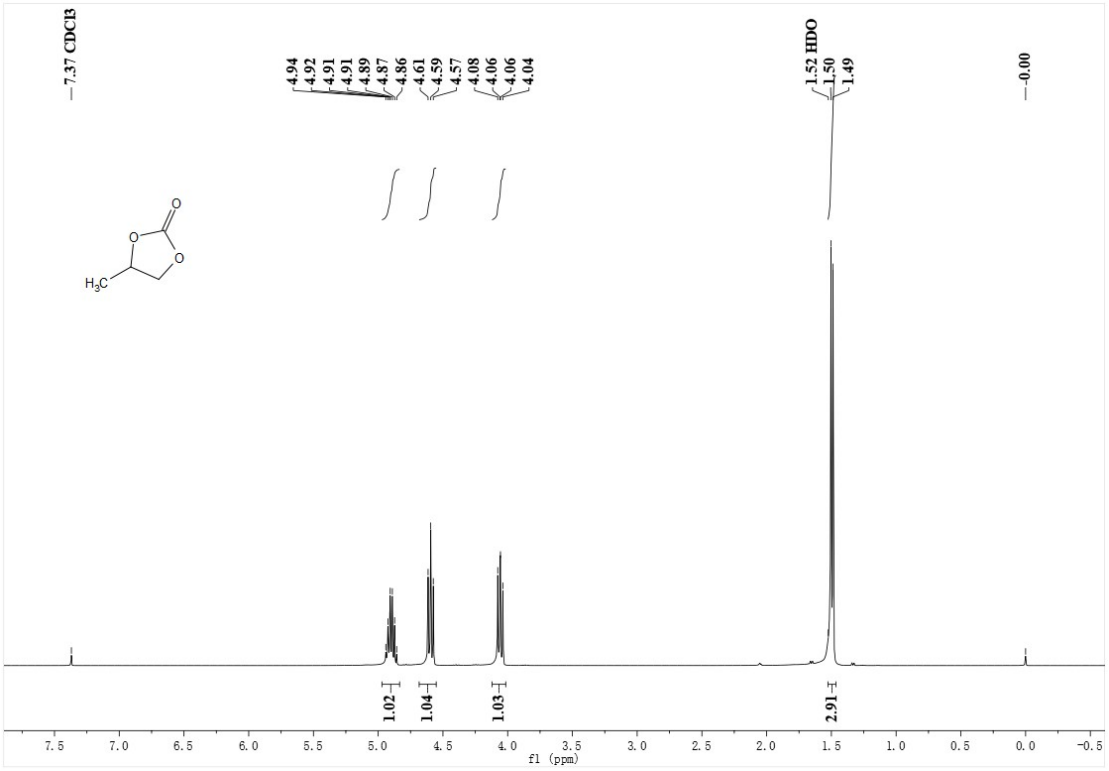

Figure S13. ^{1}H NMR spectrum of **5c**

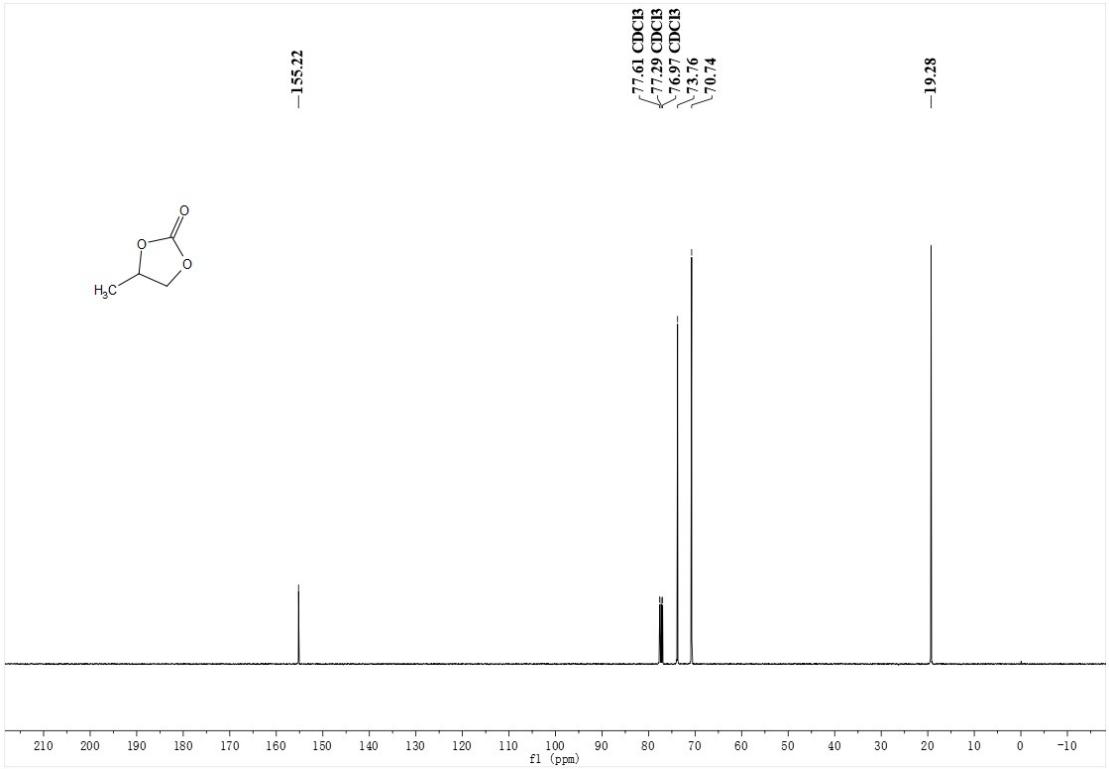

Figure S14. ^{13}C NMR spectrum of **5c**

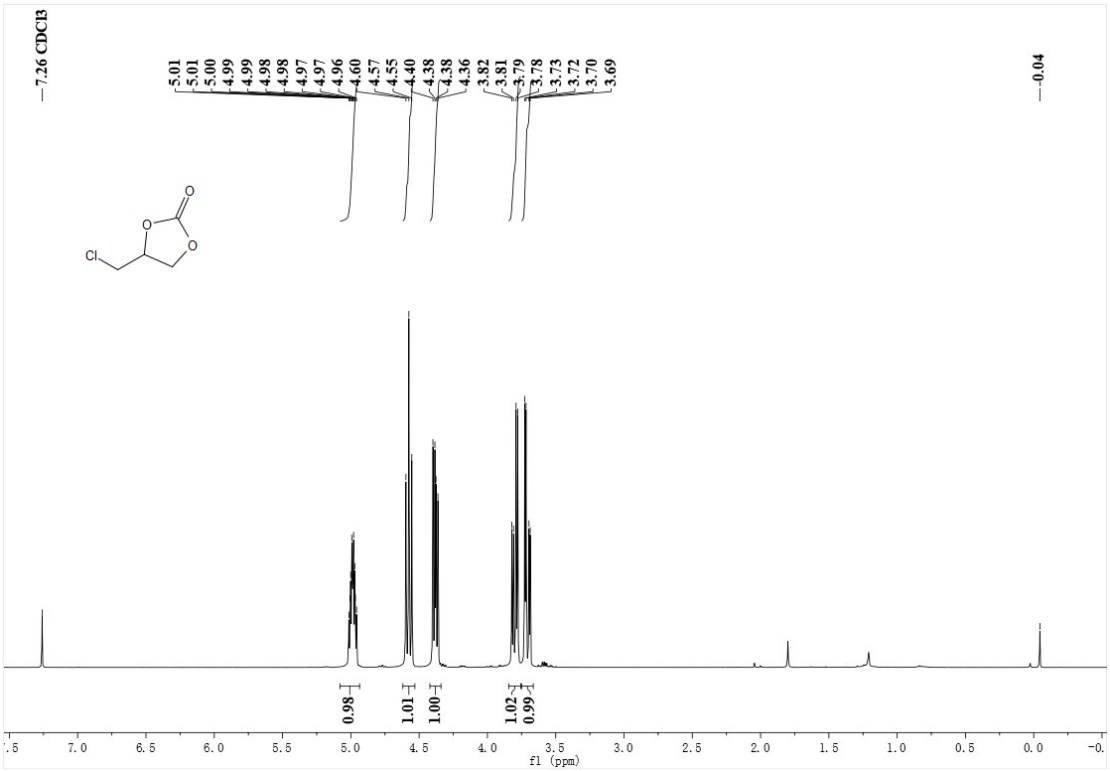

Figure S15. ^{1}H NMR spectrum of **5d**

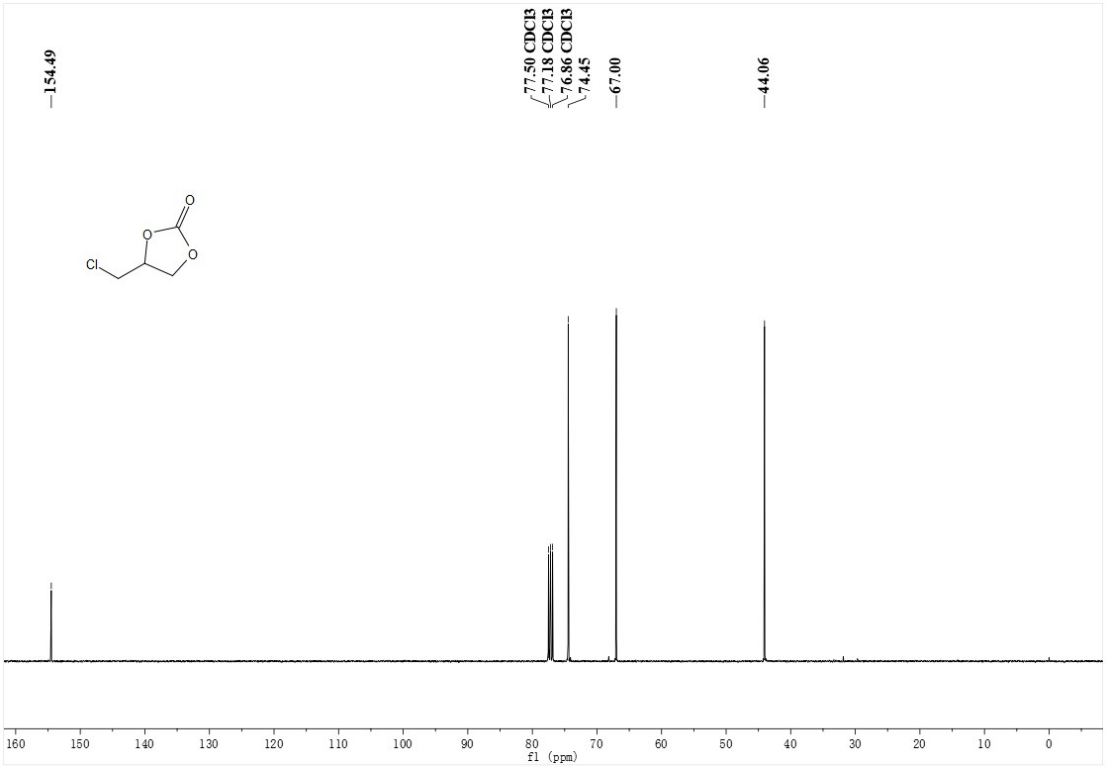

Figure S16. ^{13}C NMR spectrum of **5d**

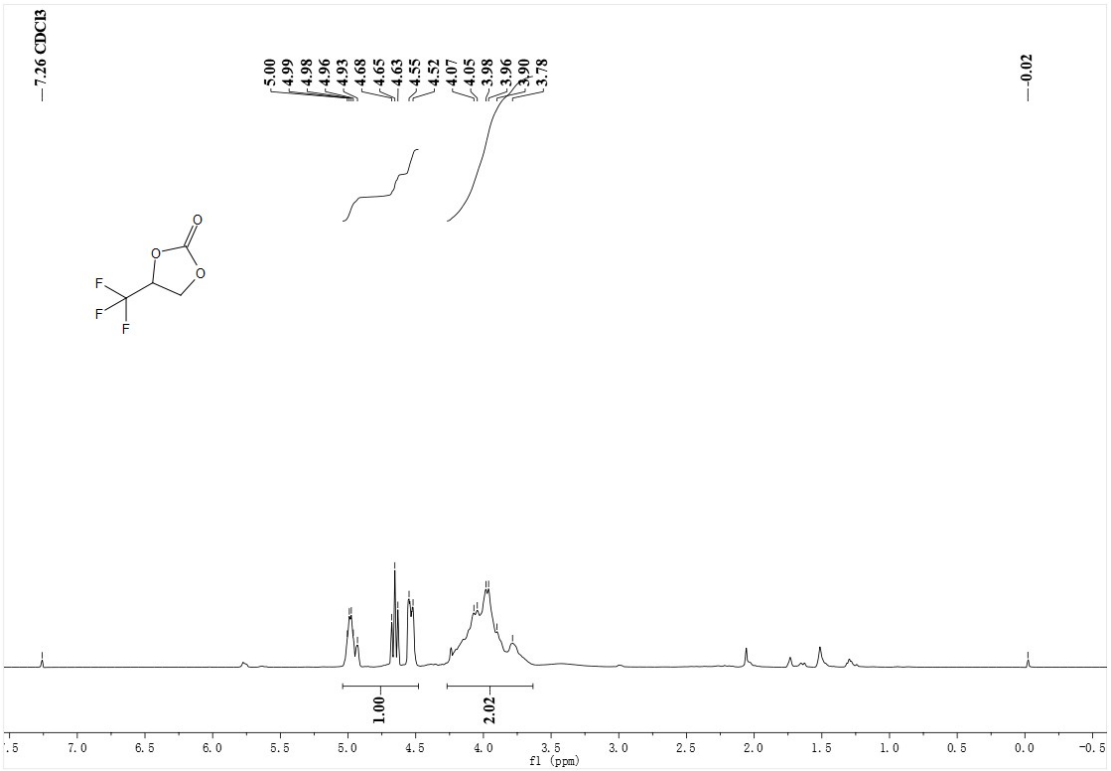

Figure S17. ^{1}H NMR spectrum of **5e**

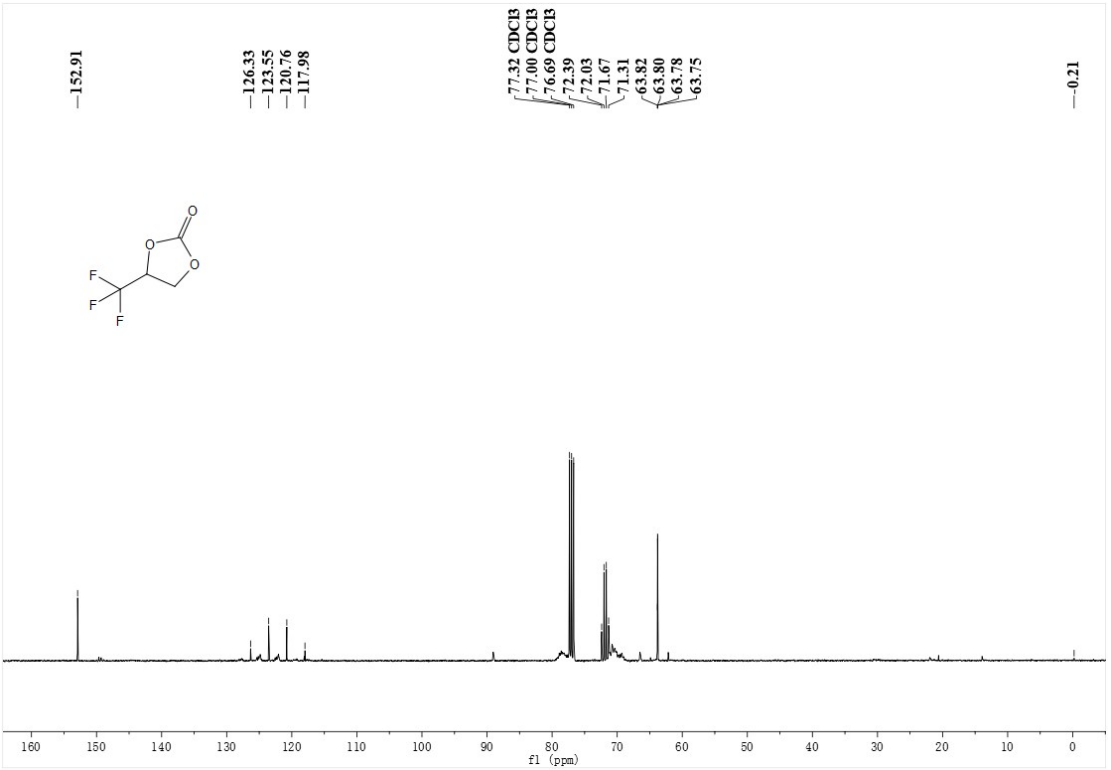

Figure S18. ^{13}C NMR spectrum of **5e**

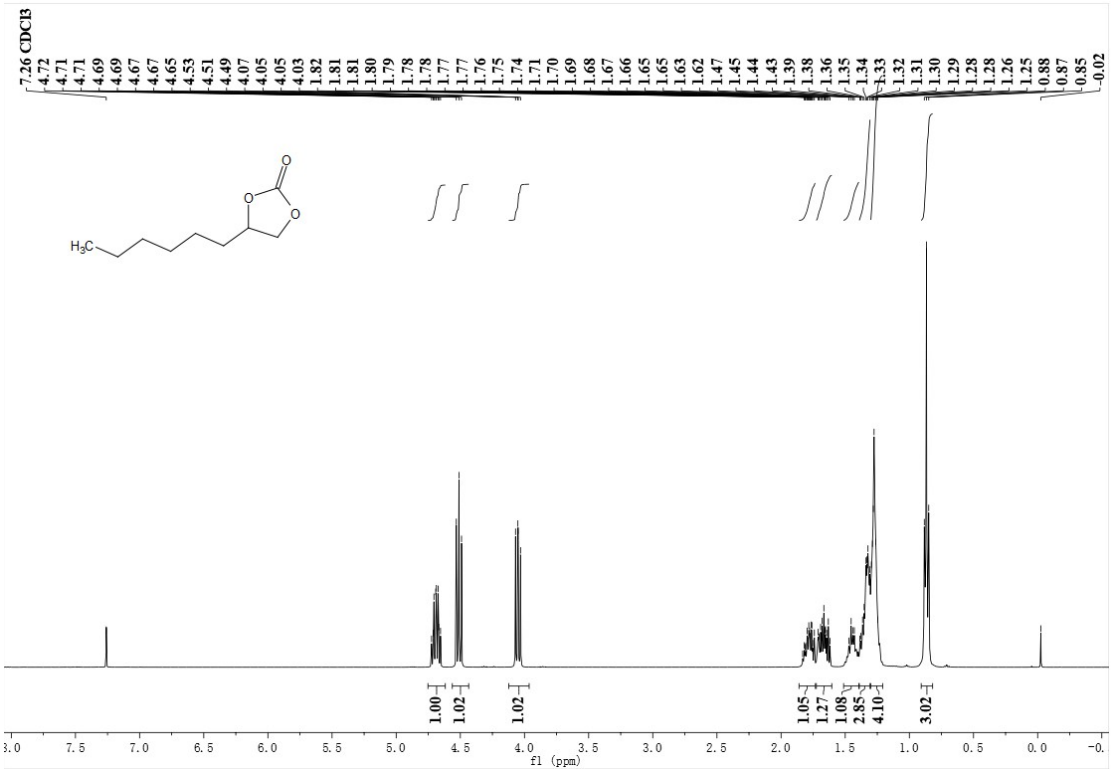

Figure S19. ^{1}H NMR spectrum of **5f**

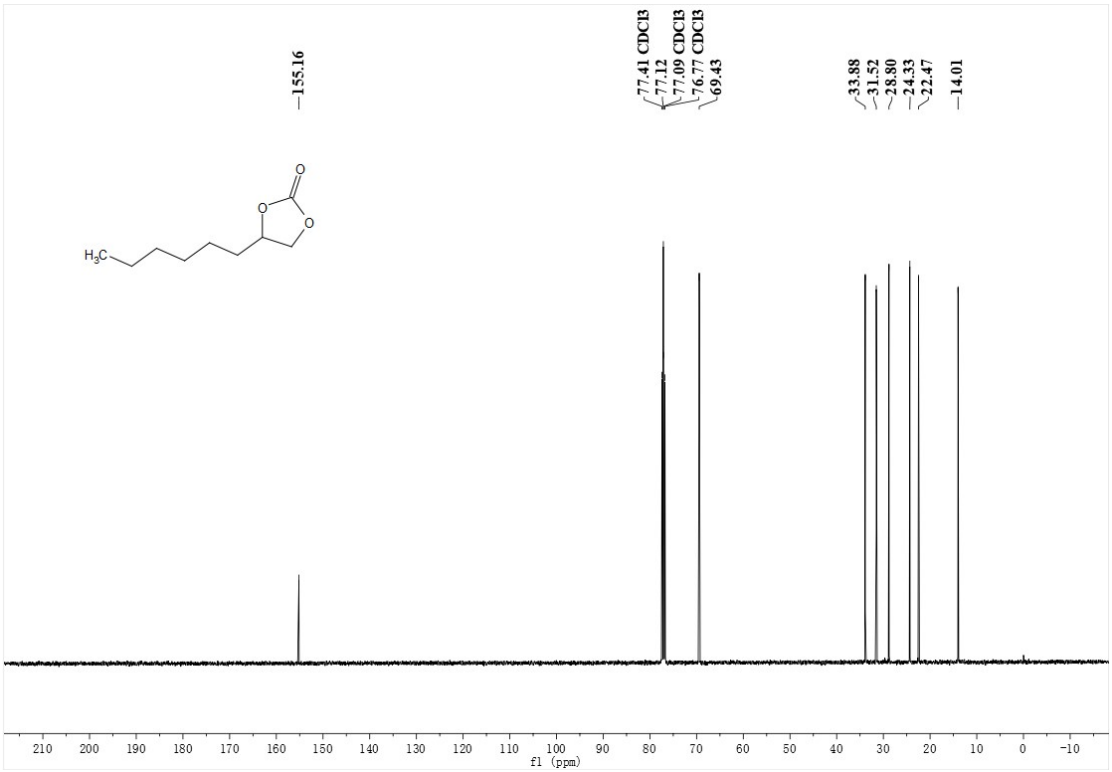

Figure S20. ^{13}C NMR spectrum of **5f**

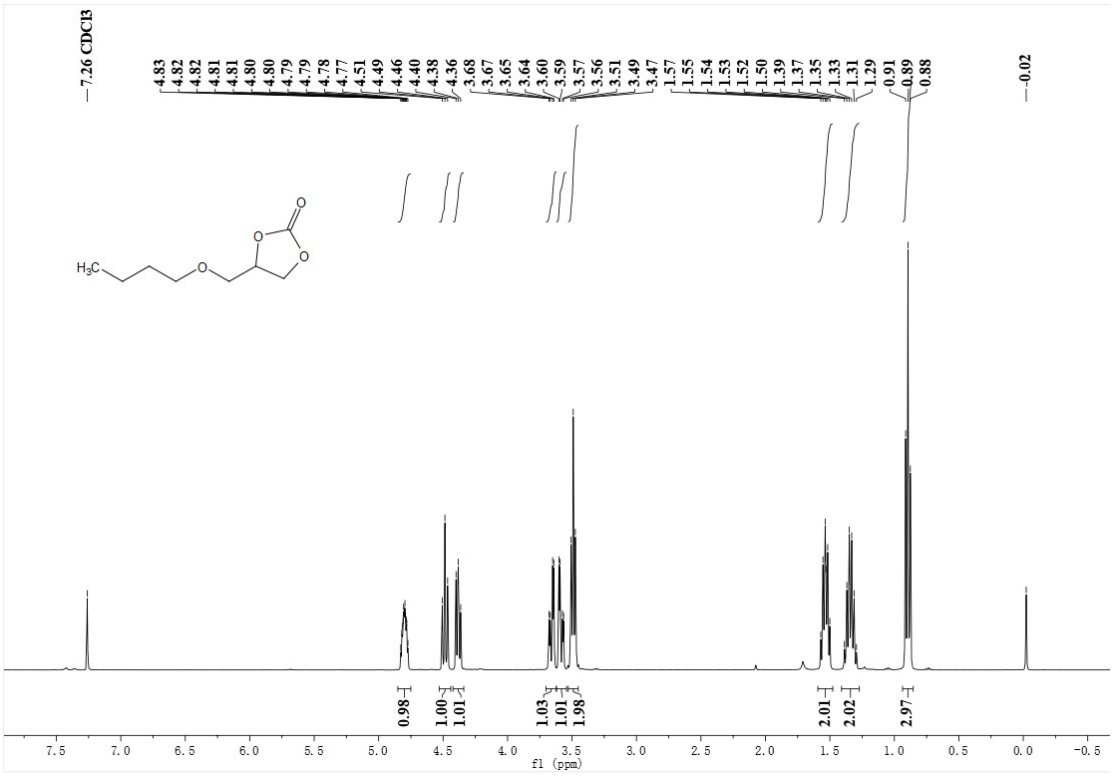

Figure S21. ^{1}H NMR spectrum of **5g**

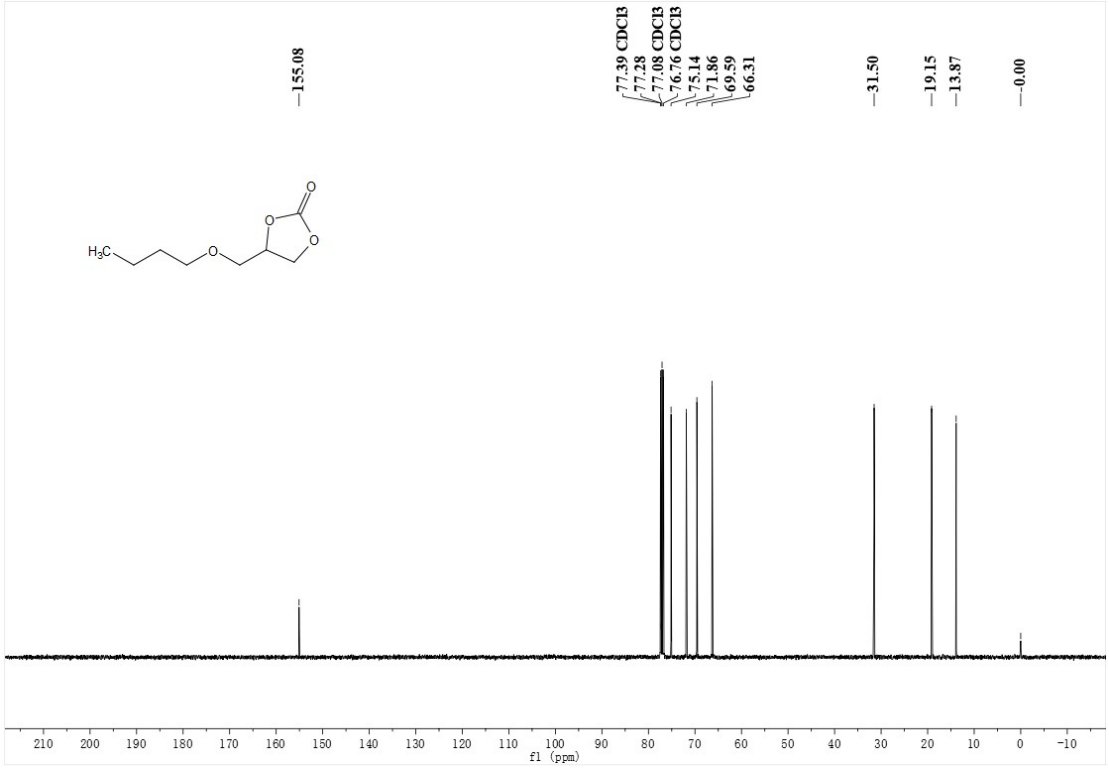

Figure S22. ^{13}C NMR spectrum of **5g**

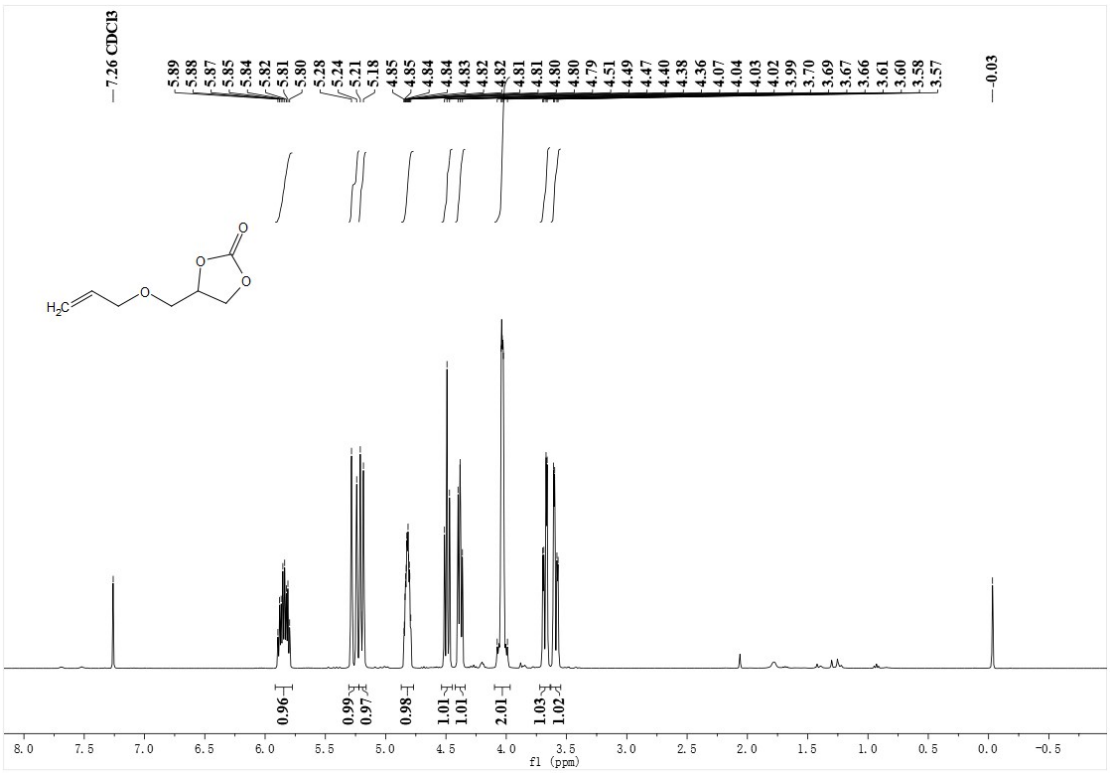

Figure S23. ^{1}H NMR spectrum of **5h**

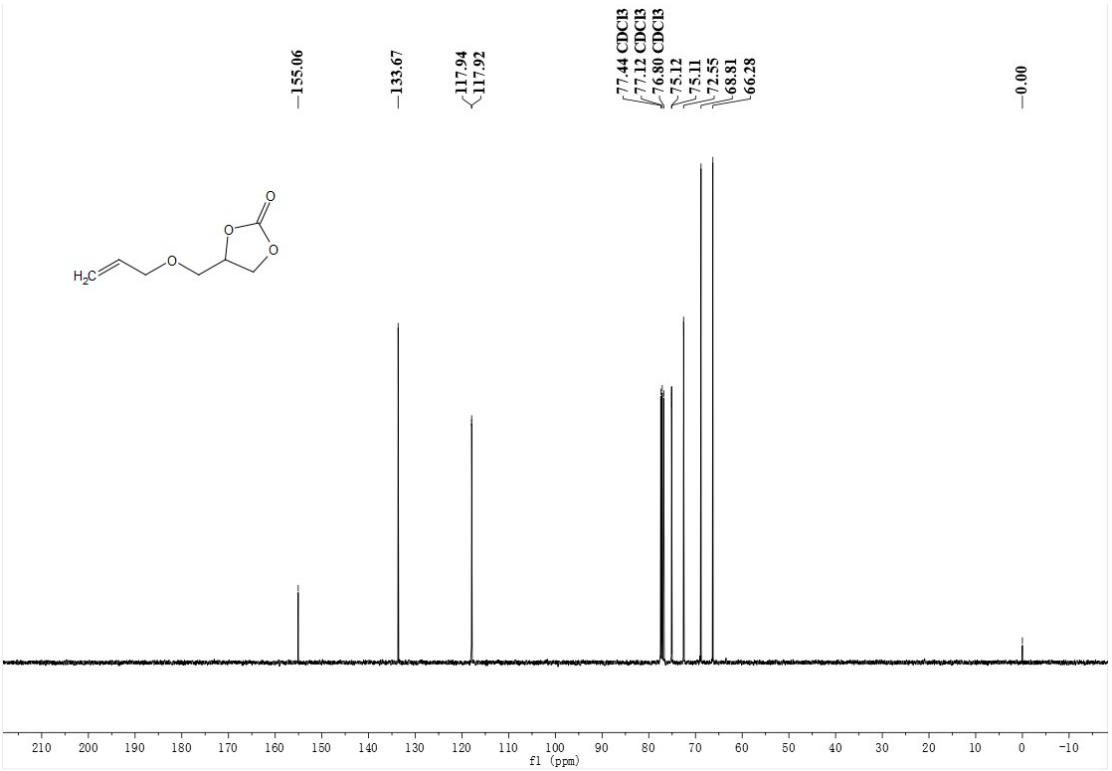

Figure S24. ^{13}C NMR spectrum of **5h**

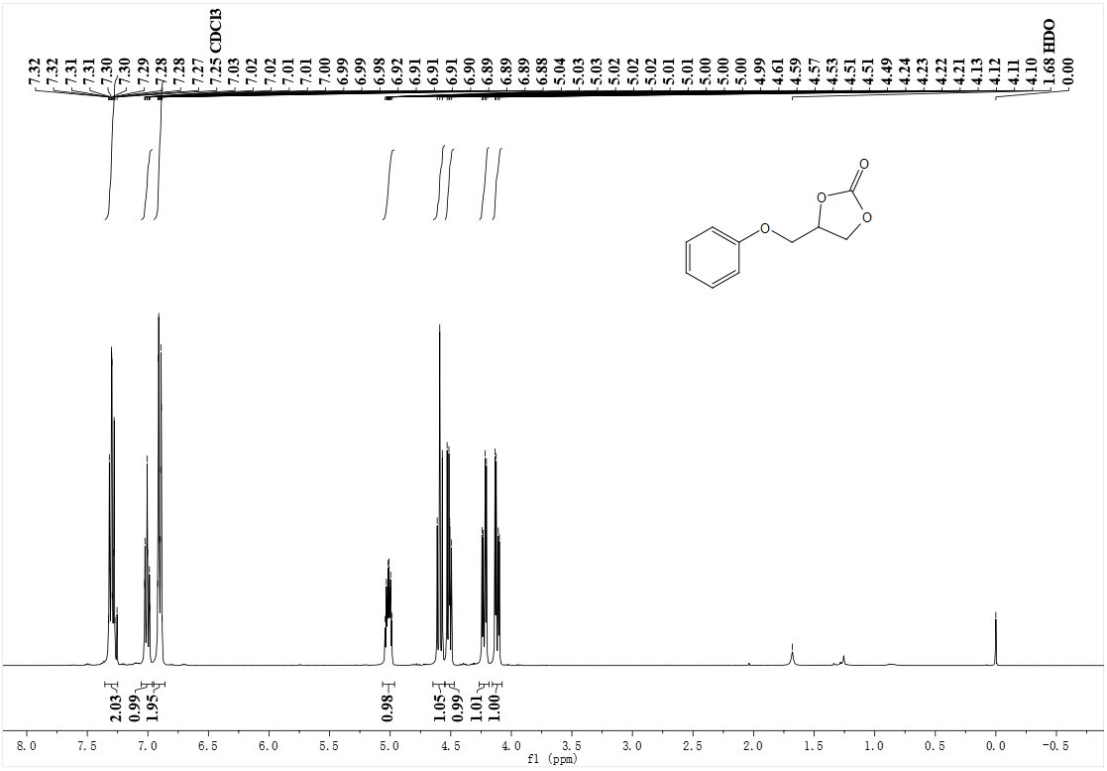

Figure S25. ^{1}H NMR spectrum of **5i**

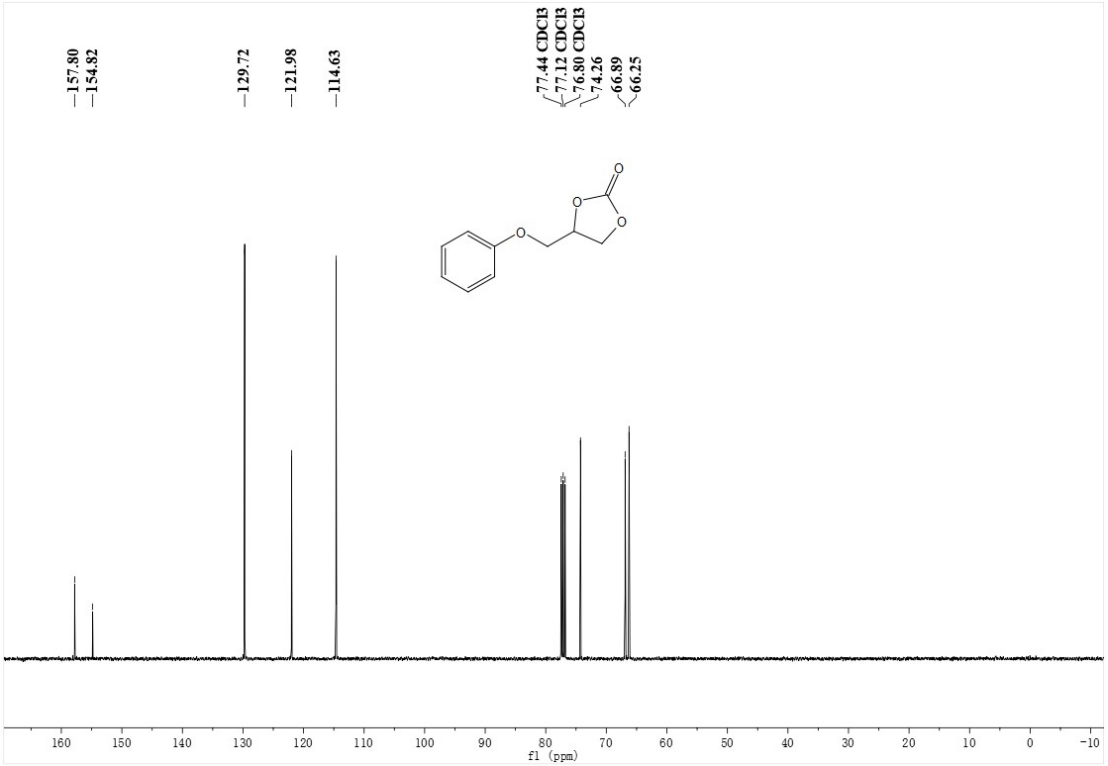

Figure S26. ^{13}C NMR spectrum of **5i**

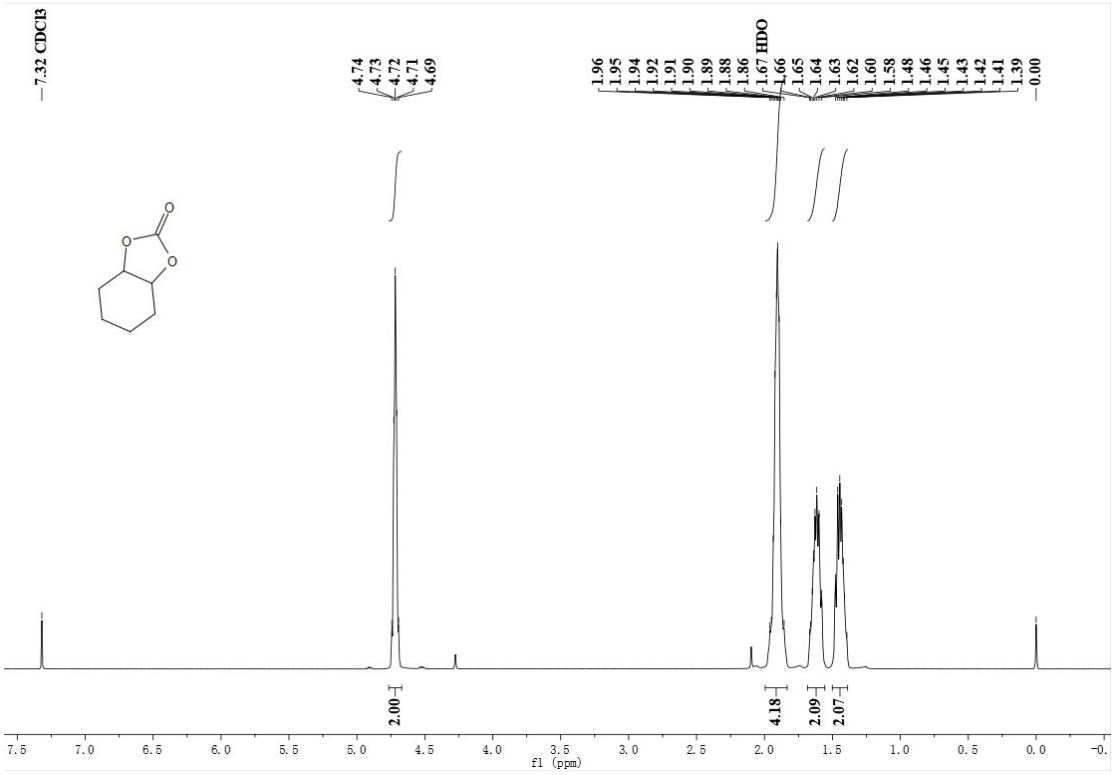

Figure S27. ^{1}H NMR spectrum of **5j**

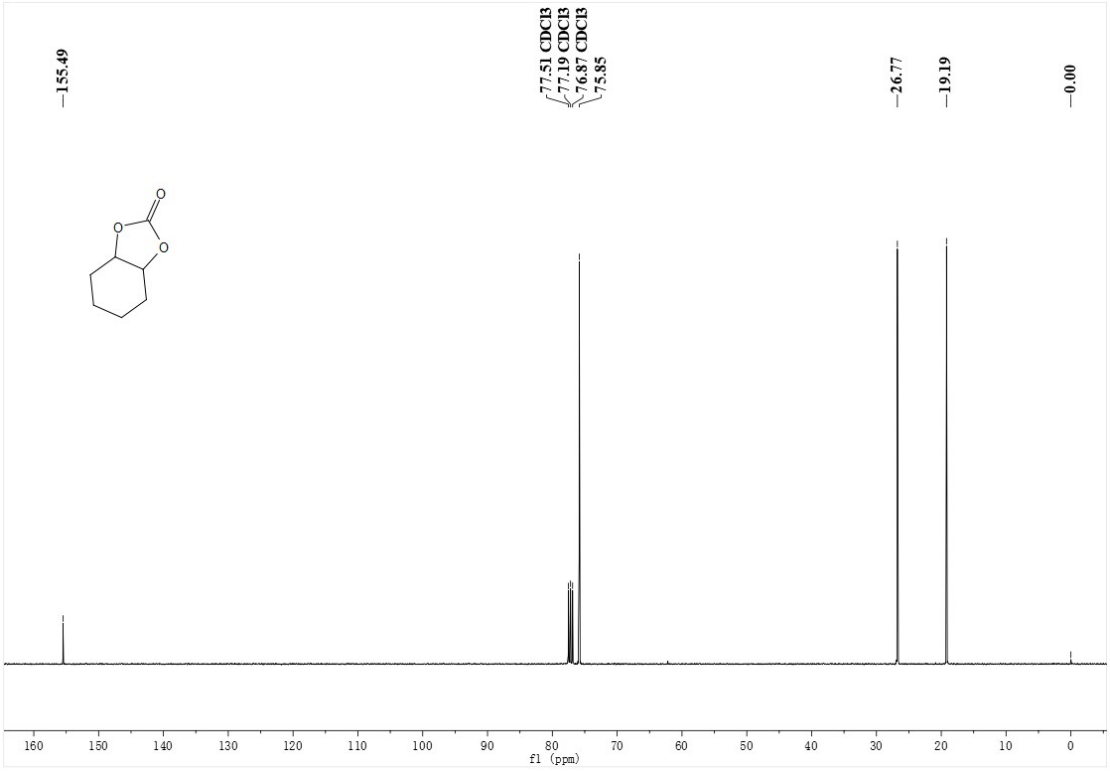

Figure S28. ^{13}C NMR spectrum of **5j**

6. Computational Methods

Geometric optimizations and frequency calculations were performed with Gaussian 16 C01.[S1] TPSSh functional[S2] was used. The def2-TZVP basis sets were used for the Co and Br atoms, and the def2-SVP basis sets were used for the other atoms.[S3-S5] Grimme's dispersion correction[4] with Becke-Johnson damping[S6] was applied. Grimme's quasi-harmonic approximation was applied to correct the entropy contribution from low-frequency vibrational modes by A single-point energy on the optimized gas phase geometry was calculated with the Model based on Density (SMD).[S7-S8] Since the epoxides were not parametrized in the SMD implementation of Gaussian 16, 1-hexanol was selected as the continuum due to its similar elemental composition and dielectric constant (ethylene oxide: 12.7 at 298.15 K;[S9] 1-hexanol: 12.51, from the Gaussian 16 SCRF definition). The electronic energies were further corrected with a single-point gas phase calculation at the PWPB95-D4[S10-S11]/def2-TZVPP level using ORCA 5.0.4.[S12] Resolution of identity (RI) approximation was applied to accelerate the computation, and the def2-TZVPP/C auxiliary basis sets[S13] were used. A −1.89 kcal/mol molar correction on the Gibbs free energy was applied to each solvated species. The wavefunction analyses were performed with Multiwfn 3.8 (dev).[S14]

5.1 Molar Correction on Gibbs Free Energies

In Gaussian 16, the Gibbs free energies are calculated under the gas phase standard state, 298.15 K and 1 atm (denoted as ΔG_p^0), even if implicit solvation model has been applied. In order to convert ΔG_p^0 to ΔG_m^0 (standard molar Gibbs free energy), we consider the chemical equation below for an associate reaction of A and B:

$A + B \rightarrow AB \cdots (Eq.S1)$

The standard Gibbs free energies can be expressed as a function of the equilibrium constant K_p or K_m:

$$\Delta G_p^0 = -RT\ln K_p = -RT\ln \frac{\frac{p(AB)}{p^0}}{\left[\frac{p(A)}{p^0}\right]\cdot\left[\frac{p(B)}{p^0}\right]} \cdots (Eq.S2)$$

$$\Delta G_m^0 = -RT\ln K_m = -RT\ln \frac{\frac{c(AB)}{c^0}}{\left[\frac{c(A)}{c^0}\right]\cdot\left[\frac{c(B)}{c^0}\right]} \cdots (Eq.S3)$$

Where $p(i)$ is the equilibrium pressure of species i, and $c(i)$ is the equilibrium constant of species i. p^0 is the normal pressure (1 atm), and c^0 is the standard concentration (1 mol/L).

Subtracting the expressions of ΔG_p^0 from ΔG_m^0 gives

$$\Delta G_m^0 - \Delta G_p^0 = -RT\ln\left\{\frac{c(AB)}{p(AB)}\cdot\left[\frac{c(A)}{p(A)}\right]^{-1}\cdot\left[\frac{c(B)}{p(B)}\right]^{-1}\cdot\left[\frac{c^0}{p^0}\right]\right\} \cdots (Eq.S4)$$

From $pV = nRT$ we have $p = (n/V)RT = cRT$. Therefore

$$\Delta G_m^0 - \Delta G_p^0 = -RT\ln\left\{(RT)^x\cdot\left[\frac{c^0}{p^0}\right]\right\} = -1.9872\times10^{-3} kcal\cdot K^{-1}\cdot mol^{-1}\cdot 298.15K\cdot\ln\left[0\right.$$
$$= -1.8943\ kcal\cdot mol^{-1} \cdots (Eq.S5)$$

Showing that a −1.89 kcal/mol correction should be applied to the Gibbs free energy for the associate reaction to refer to the correct standard state in the solution.

5.2 DFT Calculated Energies

Table S7. DFT Calculated Electronic Energies and Gibbs Free Energies (in Hartree)

	E_e(PWPB95D4)	E_e(TPSSh-D3, SMD)	E_e(TPSSh-D3, gas)	G(TPSSh-D3, gas)
Br^-	-2574.197606	-2574.227634	-2574.144560	-2574.160736
ethylene oxide	-153.745232	-153.691646	-153.687704	-153.653854
CO_2	-188.562078	-188.441547	-188.446336	-188.455361
ethylene carbonate	-342.334465	-342.176635	-342.166199	-342.118979
3b-CO	-7990.772513	-7990.509916	-7990.467756	-7989.903511
IM1	-5416.428138	-5416.261049	-5416.178454	-5415.611166
IM2	-5570.201927	-5569.974239	-5569.898258	-5569.275532
IM3	-8144.526415	-8144.214131	-8144.170077	-8143.550072
TS1	-8144.484629	-8144.200801	-8144.129600	-8143.511399
IM4	-8144.537025	-8144.223281	-8144.181757	-8143.561541
IM5	-8333.109132	-8332.677356	-8332.640849	-8332.012448
TS2	-8333.094619	-8332.672292	-8332.631071	-8332.000846
IM6	-8333.116126	-8332.695865	-8332.649865	-8332.016122
TS3	-8333.076167	-8332.667221	-8332.613186	-8331.982128
IM7	-5758.800939	-5758.461054	-5758.387488	-5757.750095

Table S8. DFT Calculated Gibbs Free Energies in the Reaction Process of 3b-Co and 3a-Co

PWPB95-D4/def2-TZVPP (SMD in 1-Hexanol) // TPSSh-D3/BS1			
3b-Co	dG(corrected)	**3a-Co**	dG(corrected)
Br-		Br-	
EO		EO	
CO2		CO2	
Co_N4_Br2	0.00	Co_N4_Br2	0.00
Co_N4_Br+	8.25	Co_N4_Br+	7.96
Co_N4_Br_EO+	8.61	Co_N4_Br_EO+	8.22
Co_N4_Br_EO_Br	7.70	Co_N4_Br_EO_Br	9.88
TS1	15.75	TS1	15.31
Co_N4_Br_OCH2CH2Br	2.76	Co_N4_Br_OCH2CH2Br	3.25
Co_N4_Br_OCH2CH2Br_CO2	5.52	Co_N4_Br_OCH2CH2Br_CO2	5.94
TS2	12.81	TS2	11.69
Co_N4_Br_OCH2CH2Br_OCO	2.66	Co_N4_Br_OCH2CH2Br_OCO	3.33
Co_N4_Br_OCH2CH2Br_OCO_iso	-0.43	Co_N4_Br_OCH2CH2Br_OCO_iso	-0.36
Co_N4_Br_OCH2CH2Br_OCO_stable	-1.48	Co_N4_Br_OCH2CH2Br_OCO_stable	-1.00
TS3	16.87	TS3	16.51
Co_N4_Br_EC+	-3.09	Co_N4_Br_EC+	-3.26
EC	-11.96	EC	-11.96

To investigate the possibility of a ring-opening mechanism involving two Co-complex molecules, DFT calculations were performed at the TPSSh-D3/def2-TZVPP(SMD, 1-hexanol)//TPSSh-D3/def2-SVP level. Assuming that the Br^- was provided by one of the Br ligand from the Co complex, the ring-opening activation barrier was calculated to be 8.96 (10.91) kcal/mol in ΔH (ΔG). In comparison, the single-Co mechanism proposed in the main text calculated at the same computational level shows a lower activation barrier of 3.90 (3.79) kcal/mol in ΔH (ΔG). Comparison of the ring-opening transition state of the two-Co (Fig S29a) and the single-Co (Fig S29b) mechanisms suggests that the irreversible ring opening occurs at a much later stage in the two-Co mechanism, as can be reflected by the longer C-O and shorter Br-C in its TS structure. This is likely due to the Br^- being bound by the source Co catalyst, and as a result, a higher activation energy is required. Furthermore, due to the low concentration of the catalyst, a two-Co mechanism would seem even less likely. We therefore would expect the single-Co mechanism to have a higher probability, as such close-binding cation-anion species (in this case, cation = $Co(N_4)Br(EO)^+$, anion = Br^-) has been commonly observed in many nucleophilic substitution reactions.

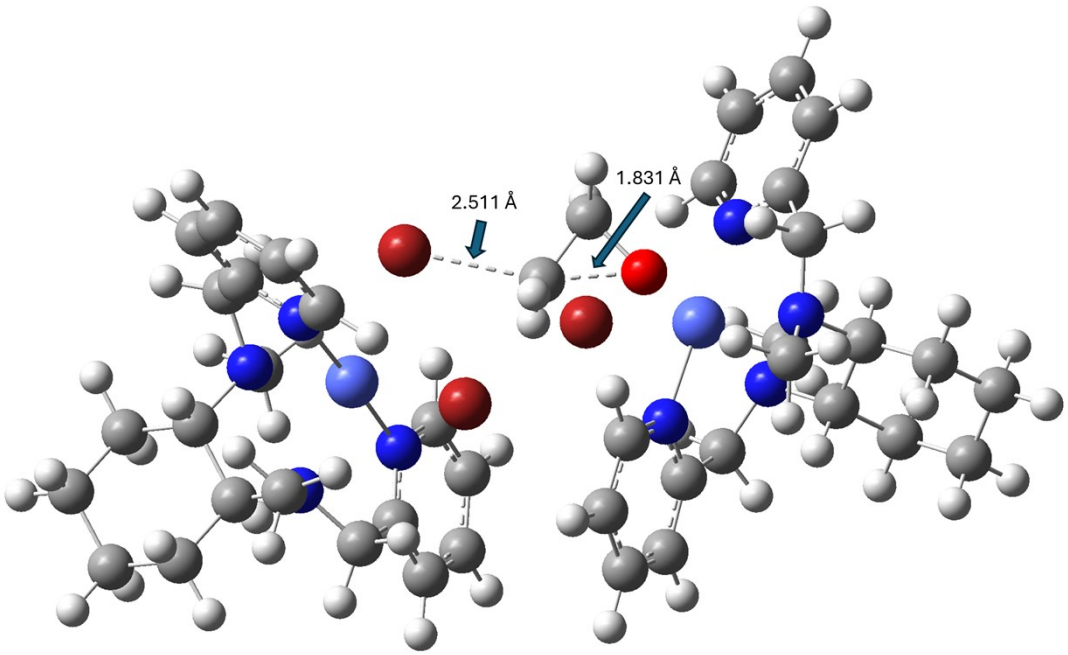

(a)

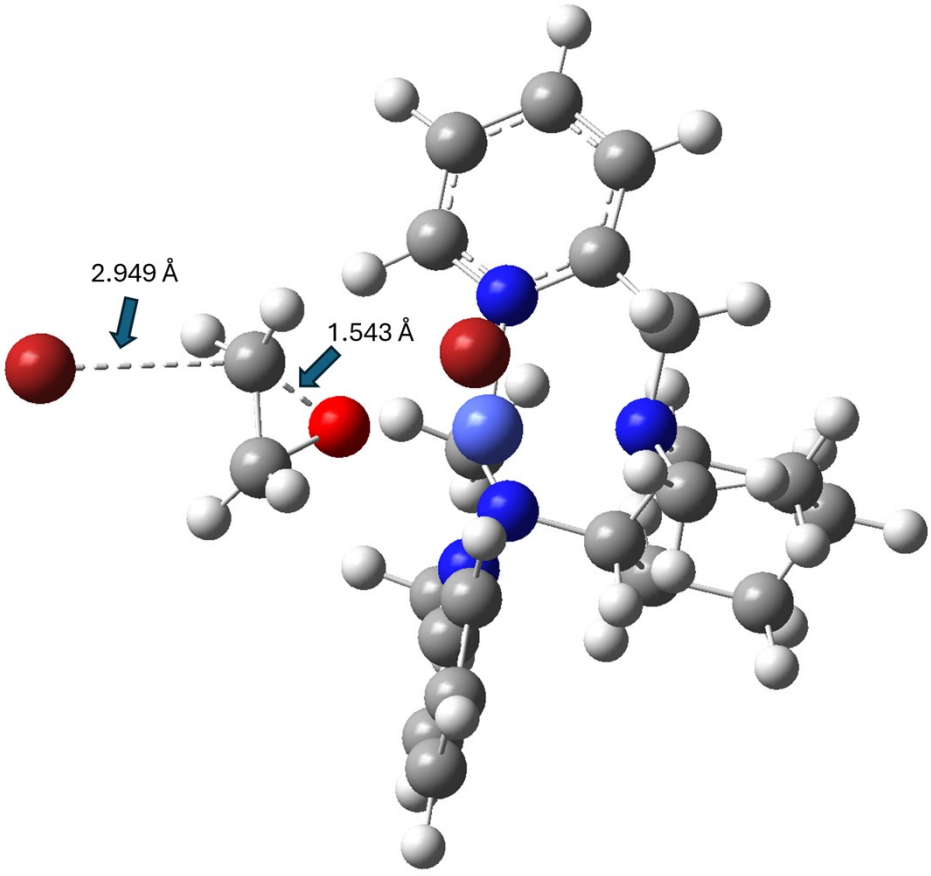

(b)

Fig S29. Ring-opening transition state structure for (a) the two-Co mechanism and (b) the single-Co mechanisms.

7. References

[S1] Gaussian 16, Revision C.01, M. J. Frisch, G. W. Trucks, H. B. Schlegel, G. E. Scuseria, M. A. Robb, J. R. Cheeseman, G. Scalmani, V. Barone, G. A. Petersson, H. Nakatsuji, X. Li, M. Caricato, A. V. Marenich, J. Bloino, B. G. Janesko, R. Gomperts, B. Mennucci, H. P. Hratchian, J. V. Ortiz, A. F. Izmaylov, J. L. Sonnenberg, D. Williams-Young, F. Ding, F. Lipparini, F. Egidi, J. Goings, B. Peng, A. Petrone, T. Henderson, D. Ranasinghe, V. G. Zakrzewski, J. Gao, N. Rega, G. Zheng, W. Liang, M. Hada, M. Ehara, K. Toyota, R. Fukuda, J. Hasegawa, M. Ishida, T. Nakajima, Y. Honda, O. Kitao, H. Nakai, T. Vreven, K. Throssell, J. A. Montgomery, Jr. J. E. Peralta, F. Ogliaro, M. J. Bearpark, J. J. Heyd, E. N. Brothers, K. N. Kudin, V. N. Staroverov, T. A. Keith, R. Kobayashi, J. Normand, K. Raghavachari, A. P. Rendell, J. C. Burant, S. S. Iyengar, J. Tomasi, M. Cossi, J. M. Millam, M. Klene, C. Adamo, R. Cammi, J. W. Ochterski, R. L. Martin, K. Morokuma, O. Farkas, J. B. Foresman, D. J. Fox, *Gaussian, Inc. Wallingford CT*., 2016.

[S2] V. N. Staroverov, G. E. Scuseria, J. Tao, J. P. Perdew, *J. Chem. Phys.*, 2003, **119**, 12129–12137.

[S3] F. Weigend, R. Ahlrichs, *Phys. Chem. Chem. Phys.*, 2005, **7**, 3297–3305;

[S4] F. Weigend, *Phys. Chem. Chem. Phys*, 2006, **8**, 1057–1065.

[S5] S. Grimme, J. Antony, S. Ehrlich, H. Krieg, *J. Chem. Phys.*, 2010, **132**, 154104.

[S6] S. Grimme, S. Ehrlich, L. Goerigk, *J. Comput. Chem.*, 2011, **32**, 1456–1465.

[S7] S. Grimme, *J. Chem. Eur.*, 2012, **18**, 9955–9964;

[S8] A. V. Marenich, C. J. Cramer, D. G. Truhlar, *J. Phys. Chem.*, 2009, **113**, 6378–6396.

[S9] S. Kozuch, J. M. Martin, *J. Comput. Chem.*, 2013, **34**, 2327–2344.

[S10] D. W. Davidson, G. J. Wilson, *Can. J. Chem.*, 1963, **41**, 1424–1434;

[S11] E. Caldeweyher, C. Bannwarth, S. Grimme, *J. Chem. Phys.*, 2017, **147**, 034112.

[S12] F. Neese, F. Wennmohs, U. Becker, C. Riplinger, *J. Chem. Phys*., 2020, **152**, 224108.

[S13] A. Hellweg, C. Hättig, S. Höfener, W. Klopper, *Theor. Chem*. *Acc.*, 2007, **117**, 587–597.

[S14] T. Lu, F. Chen, *J. Comput. Chem*., 2012, **33**, 580–592.